Gapless Quantum Spin Liquid in an Organic Spin-1/2 Triangular-Lattice $\kappa - H_3(Cat\text{-}EDT\text{-}TTF)_2$

Takayuki Isono,[1] Hiromichi Kamo,[1] Akira Ueda,[1] Kazuyuki Takahashi,[2] Motoi Kimata,[1] Hiroyuki Tajima,[1] Satoshi Tsuchiya,[3] Taichi Terashima,[3] Shinya Uji,[3] and Hatsumi Mori[1]

[1]*The Institute for Solid State Physics (ISSP), The University of Tokyo, Kashiwa, Chiba 277-8581, Japan*

[2]*Department of Chemistry, Kobe University, Kobe, Hyogo 657-8501, Japan*

[3]*National Institute for Materials Science, Tsukuba, Ibaraki 305-0003, Japan*

(Received 9 June 2013; revised manuscript received 14 April 2014; published 30 April 2014)

We report the results of SQUID and torque magnetometry of an organic spin-1/2 triangular-lattice $\kappa - H_3(Cat\text{-}EDT\text{-}TTF)_2$. Despite antiferromagnetic exchange coupling at 80–100 K, we observed no sign of antiferromagnetic order down to 50 mK owing to spin frustration on the triangular lattice. In addition, we found nearly temperature-independent susceptibility below 3 K associated with Pauli paramagnetism. These observations suggest the development of gapless quantum spin liquid as the ground state. On the basis of a comparative discussion, we point out that the gapless quantum spin liquid states in organic systems share a possible mechanism, namely the formation of a band with a Fermi surface possibly attributed to spinons.

DOI: 10.1103/PhysRevLett.112.177201 PACS numbers: 75.10.Kt, 75.30.Gw, 75.40.Cx

A quantum spin-liquid (QSL) state is an exotic ground state where interacting spins continue to fluctuate without any formation of long-range magnetic order (LRMO) even at a sufficiently low temperature [1–4]. Such a liquid can exist when quantum-mechanical fluctuations of spins are dominant and, thus, destabilize the conventional LRMO. In one-dimensional spin systems with $S = 1/2$, the nature of the QSL states is thoroughly described by $S = 1/2$ fractionalized particles (spinons) as elementary excitations [4,5]. Conversely, in the case of two or more dimensions, a variety of QSL states have been theoretically predicted [1,6–15], but nevertheless, a systematic understanding of the elementary excitation from the experiments remains an arduous challenge. This is mainly because of the rareness of the experimental candidates, which are still restricted to the several spin-frustrated lattices, such as triangular [16–19], kagome [20], and hyperkagome lattices [21].

Among the candidates, the organic spin-1/2 triangular lattices, $\kappa - (BEDT\text{-}TTF)_2Cu_2(CN)_3 (\kappa - CN)$ and $\beta' - EtMe_3Sb[Pd(dmit)_2]_2 (\beta' - Sb)$, have been intensively studied. In these materials, an $S = 1/2$ spin is distributed on a site of the two dimensional (2D) triangular lattice, and interacts with the nearest neighbors by antiferromagnetic Heisenberg exchange coupling. In spite of the large coupling constant $J/k_B \sim 250$ K, there is no LRMO down to the low temperature $T \sim 20$ mK, that is, $\sim(J/k_B)/10^4$ [16,17,22–25]. This observation indicates that the spin fluctuation enhanced by the competing exchange interactions prevents the formation of long-range antiferromagnetic order, leading to the emergence of the QSL state. One notable result for the QSL state is that each elementary excitation spectrum seems to be quite different. The QSL state in β'-Sb is characterized by gapless magnetic excitations, as indicated by the presence of the T-linear term of the specific heat and the thermal conductivity [23,26], and T-independent susceptibility [27], for $T \to 0$: characteristics of a Fermi liquid. In the case of κ-CN, however, the existence of gapless excitations has been suggested by measurement of the specific heat [24], whereas thermal conductivity and muon spin rotation have revealed the opening of a tiny gap in the excitation spectrum [25,28]. The apparent discrepancy between the gapless and gapped features has been explained by the microscopic phase separation into paramagnetic and nonmagnetic phases [29]. Here, a next important step towards the elucidation of the QSL in the organic spin-1/2 triangular lattices is to reveal the universal nature of the excitation spectrum for the QSL states. To this end, the experimental realization of the novel candidates is an urgent necessity.

Recently, we successfully synthesized a 2D organic Mott insulator $\kappa - H_3(Cat\text{-}EDT\text{-}TTF)_2 (\kappa - H)$ [30]. A characteristic structural feature of this material is that, in a 2D layer, two face-to-face $(H_2Cat\text{-}EDT\text{-}TTF)^{0.5+}$ molecules form a strongly dimerized molecular unit, as shown in Fig. 1(a). Because of the strong dimerization, a dimerized unit can be treated as one site, resulting in an effective spin 1/2 per site. As schematically illustrated in Fig. 1(b), each spin is arranged on the triangular mesh with the anisotropy parameter $t'/t \sim 1.48$ at $T = 50$ K, where t and t' are the hopping integrals around the sides of rhomboids and along one diagonal, respectively. The moderately one-dimensional anisotropy is clearly distinct from $t'/t \sim 0.8$–0.9 of other organic QSL materials [31–35]. In this Letter, we report the results of SQUID and torque magnetometry suggesting the QSL state with gapless magnetic excitations in κ-H. A comparison of magnetic properties among organic QSL materials would provide important information on a possible mechanism of the gapless QSL states: the

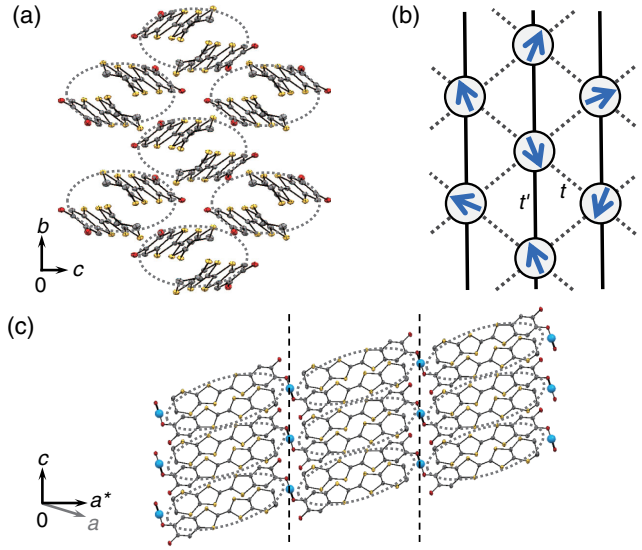

FIG. 1 (color online). (a) Molecular arrangement in a two-dimensional layer (b-c plane) of κ-H. The dotted ellipsoids denote the strongly dimerized molecules. (b) A schematic of the anisotropic triangular lattice with transfer integrals t' and t. The closed circles and the arrows on them represent the sites of the triangular lattice composed of the dimerized molecules and the $S = 1/2$ spins, respectively. (c) The interlayer packing structure viewed in the a-c plane. The adjacent layers are connected by hydrogen bonds. The dotted ellipsoids represent dimerized molecules similar to those described in (a).

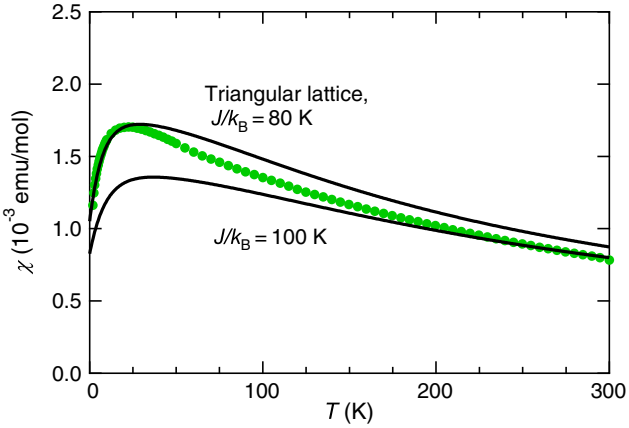

FIG. 2 (color online). Static magnetic susceptibility as a function of temperature $\chi(T)$. The closed circles represent data of susceptibility. The solid lines denote the susceptibility curve based on the $S = 1/2$ Heisenberg antiferromagnetic model of an isotropic triangular lattice with an exchange-coupling constant $J/k_B = 80$ and 100 K (Refs. [38,39]).

formation of a band with a Fermi surface possibly attributed to spinons.

Samples were prepared by the electrochemical oxidation of H_2Cat-EDT-TTF molecules in the presence of a base [30,36]. For poly-crystalline samples of ~16 mg, we measured the static magnetic susceptibility at 1 T employing a magnetic property measurement system (Quantum Design) in the temperature region from 2 to 300 K. The diamagnetic contribution was corrected using Pascal's law. The magnetic properties of three distinct crystals (#1, 2, and 3) below 2 K were probed by torque magnetometry, adopting a microcantilever [37]. The high sensitivity of this method allowed the detection of a considerably weak signal of the paramagnetic torque on a single crystal with typical mass less than 0.7 μg. All the torque measurements were made using a 20 T superconducting magnet with a dilution refrigerator down to $T = 50$ mK at Tsukuba Magnet Laboratories, NIMS.

Temperature dependence of the static magnetic susceptibility $\chi(T)$ is presented in Fig. 2. As temperature decreases, $\chi(T)$ monotonically increases and takes a broad maximum around $T \sim 20$ K. On further cooling, although $\chi(T)$ turns to decrease rapidly, there is no clear evidence of a magnetic transition down to 2 K. Instead, the maximum of χ observed at $T \sim 20$ K points to the development of an antiferromagnetic correlation without any LRMO. The entire temperature dependence of χ is roughly described by the $S = 1/2$ Heisenberg antiferromagnetic model of an isotropic triangular lattice [38,39], with an antiferromagnetic exchange-coupling constant $J/k_B \sim$ 80–100 K. This result indicates that the spin frustration derived from the geometry of the triangle is inherent in the system, and profoundly affects the magnetic properties.

To shed light on the magnetic properties at lower temperatures, we measured the magnetic torque. As the magnetic torque only detects the anisotropic susceptibility in principle, the isotropic contribution from impurity spins is naturally eliminated, providing us with the intrinsic low-temperature magnetic properties. Figure 3(a) and 3(b) shows the magnetic torque as a function of the field angle $\tau(\theta)$ measured at $T = 0.4$ K, with the field rotation in the a^*–b and a^*–c planes [see Figs. 1(a) and 1(c)], respectively. For both rotations, one finds a sinusoidal angular variation in τ, following an expression $\tau(\theta) = A \sin 2(\theta + \theta_0)$, as shown by the solid lines in the figures. Here, A and θ_0 represent the amplitude and phase factor of the sinusoidal function, respectively. Similar sinusoidal behavior is observed at all temperatures (down to $T \sim 50$ mK) and field strengths (up to $H = 17$ T) investigated. As shown by the arrows in Figs. 3(a) and 3(b), the phase factor θ_0 gradually shifts with an increase in the magnetic field, simultaneously with a pronounced enhancement of the amplitude A of the sinusoidal function. The detail of the phase shift for a^*–b and a^*–c rotations is summarized as the field dependence of θ_0 for the various temperatures and samples in Figs. 3(c) and 3(d), respectively. Below 4 K, in the weak-field regime, θ_0 is continuously modified by the magnetic field, while θ_0 is little affected by the field above ~11 T, at which the phase shift reaches approximately 10°–20°. At 15 K, however, θ_0 has weak field dependence up to 17 T, indicating that the phase shift occurs at temperatures lower than 15 K. The field evolution of the amplitude $A(H)$ of the sinusoidal torque curve is presented in Fig. 3(e) and its inset. For both field rotations, $A(H)$ increases rapidly with respect to the applied field, which is

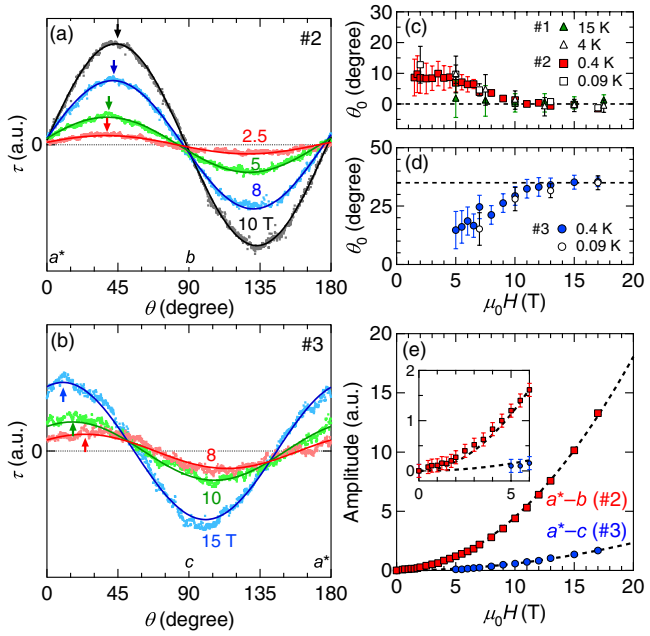

FIG. 3 (color online). Field-angle dependence of the magnetic torque $\tau(\theta)$ at 0.4 K, with field rotation in (a) a^*–b and (b) a^*–c planes. The solid line shows a double-angle function $\tau(\theta) = A \sin 2(\theta + \theta_0)$, where A and θ_0 denote the amplitude and phase factor. The arrows represent the field angle for maximum τ. For clarity, not all the measurement data are shown. The field dependence of the phase factor $\theta_0(H)$ for (c) a^*–b and (d) a^*–c rotations and the various samples and temperatures. (e) The field evolution of the amplitude $A(H)$ of the torque curve at 0.4 K. The dashed line shows a quadratic function $A(H) = BH^2$ with a certain coefficient B. Inset: an enlarged figure for the weak-field regime. $\tau(\theta)$ and $A(H)$ are presented in arbitrary units.

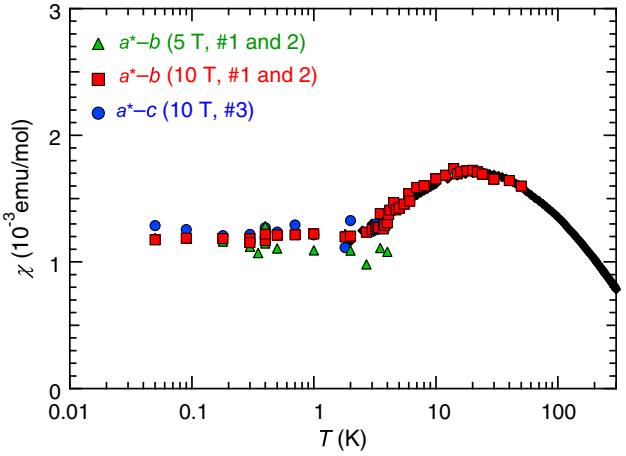

FIG. 4 (color online). Magnetic susceptibility as a function of temperature $\chi(T)$ on a semilogarithmic plot. The diamonds denote the result of the SQUID measurement at 1 T. The triangles, squares, and circles represent $\chi(T)$ estimated from the torque at 5 and 10 T for a^*–b rotation, and at 10 T for a^*–c rotation, respectively. The susceptibility $\chi(T)$ for the a^*–b and a^*–c rotations is normalized to $\chi(50\ \mathrm{K})$ and $\chi(4\ \mathrm{K})$ from the SQUID measurement, respectively.

strictly described by a quadratic function $A(H) = BH^2$ with a certain coefficient B.

On the basis of the results of the SQUID and the torque magnetometry, let us first discuss whether LRMO develops in κ-H. In general, magnetic torque in paramagnetic states is characterized by a sinusoidal variation with twofold periodicity in regard to the field angle, and an amplitude proportional to the square of the field: $\tau_{ij}(\phi) = [M \times H]_k = (1/2)\Delta\chi H^2 \sin 2\phi$ for field rotation in the i-j plane. Here, $M_i (= \chi_i H_i)$, $\Delta\chi (= \chi_i - \chi_j)$, and ϕ denote the magnetization along the crystallographic i axis, the magnetic anisotropy, and the angle between the field and the i axis, respectively. In the case of simple antiferromagnets below the Néel temperature, the angular variation in the torque has similar sinusoidal behavior reflecting uniaxial magnetic anisotropy in the sufficiently weak-field regime. In contrast, for the wide-field regime approximately above the spin-flop field, the magnetic moment induced by the field along or close to the magnetic easy axis gives rise to an additional contribution to the torque signal, resulting in the drastic change in the shape of the torque curve [40,41]. For our system, it should be noted that sinusoidal behavior with twofold periodicity is observed up to $H = 17$ T and down to $T = 50$ mK, and the behavior above 11 T corresponds to what is expected from anisotropy of the g factor at room temperature [42]. Moreover, the observed amplitude of the sinusoidal torque curve is precisely proportional to the square of the magnetic field. These observations indicate that the system remains paramagnetic even at $T = 50$ mK. The above argument about the torque together with the susceptibility $\chi(T)$ reveals that spin frustration on the triangular lattice strongly suppresses the formation of long-range antiferromagnetic order even at $T \sim (J/k_B)/10^3$, suggesting the development of the QSL state as the ground state.

Second, we focus on the excitation spectrum of the QSL state. Recently, Watanabe *et al.*. revealed that the absolute value of the susceptibility of QSL states can be determined from the magnetic torque, under the assumption that the susceptibility is proportional to the square of the g factor, similar to the case for conventional paramagnets [27]. Employing their methodology reported in Ref. [27], we estimated the magnetic susceptibility $\chi(T)$ down to 50 mK, where we assumed that the g factor is little affected by cooling (see also, Supplemental Material [43]). The estimated $\chi(T)$ is plotted as a function of temperature in Fig. 4. Here, $\chi(T)$ is normalized using the averaged χ determined from the SQUID measurement at the highest temperature of the torque magnetometry, because the very small mass of the single crystals makes the accurate estimation of χ difficult. The normalization is ensured by the markedly small anisotropy in the g factor of ~0.25%; χ along a certain axis little deviates from the average χ. In fact, the susceptibility falls on an identical curve in the wide-temperature regime from 50 K to 50 mK. What is notable in Fig. 4 is that $\chi(T)$ is nearly independent of temperature below $T \sim 3$ K. In general, the T independence of

susceptibility for paramagnetic states derives from the van Vleck and Pauli paramagnetic contribution. In organic materials composed of light atoms, the van Vleck contribution is usually sufficiently small as to be negligible (see, for example, Ref. [27]). The Pauli contribution depends on the density of states $D(E_F)$ at the Fermi level. In the case of β'-Sb, observations of the T-linear term of the specific heat and the thermal conductivity for $T \to 0$ [23,26], in addition to the T-independent susceptibility [27], have provided circumstantial evidence that $D(E_F)$ is caused by fermionic quasiparticles of the QSL state. Taking the analogy of β'-Sb, the T-independent susceptibility observed for κ-H can possibly be attributed to the Pauli paramagnetic contribution. This suggests the presence of gapless magnetic excitations in the QSL state.

The discovery of the third candidate for the QSL state offers us the first opportunity to reveal the universal nature of the gapless QSL states in organic spin-1/2 triangular lattices, on the basis of a comparative discussion. Next, let us compare and discuss the gapless QSL states of κ-H and β'-Sb. Table 1 compares the anisotropy parameter t'/t of the triangles, the exchange-coupling constant J/k_B, and the Pauli paramagnetic susceptibility χ_0 between κ-H and β'-Sb. One immediately notices that t'/t differs between the two materials. Moreover, χ_0 for κ-H is found to be three times that for β'-Sb, whereas J/k_B for κ-H is about one-third that for β'-Sb. In general, the Pauli susceptibility χ_0 is proportional to $D(E_F)$. Additionally, in a simple band picture, $D(E_F)$ is inversely related to the band width, which corresponds to the energy scale of interactions, namely, the exchange coupling J in the present case. Therefore, χ_0 is expected to be proportional to the reciprocal of J. Surprisingly, this simple consideration based on the band picture fully explains the magnitude relation of χ_0 and J/k_B between κ-H and β'-Sb. This finding together with the distinct t'/t for κ-H and β'-Sb allows two remarkable suggestions to be made: (1) Gapless QSL states in the organic spin-1/2 triangular lattices emerge in the wide-parameter range of t'/t; (2) such QSL states are systematically understood within one framework, that is, the formation of a band with a Fermi surface derived from fermionic quasiparticles.

Suggestion (2) appears to be consistent with the theory in which spinons as fermionic quasiparticles are responsible for the QSL state with a Fermi surface [9–11,44–48]. Many of the cited studies have pointed out that the charge fluctuation inherent in organic triangular lattices plays an important role for the QSL state [9,10,46–48]. As the organic triangular lattices are usually located in the vicinity of the Mott transition, the slight probability of the charge carriers hopping to the neighboring sites inevitably remains, leading to the charge fluctuation. In theoretical studies, such fluctuations are treated as ring-exchange interactions, which stabilize the QSL state with the spinon Fermi surface [9,10]. Because of the gapless spinon excitation over the entire Fermi surface, χ_0 is expected to approach a constant value as the temperature goes to zero: $\chi_0 \sim 0.28\mu_B^2/t_{spinon}$ for the triangular lattice [9]. From the experimental values of χ_0, the hopping amplitudes t_{spinon} of spinons are estimated as ~90 and 260 K for κ-H and β'-Sb, respectively, which clearly coincide with J/k_B. This suggests that $D(E_F)$ observed for the gapless QSL states is derived from spinons.

TABLE I. Comparison of the anisotropy parameter t'/t, the exchange coupling constant J/k_B, and the temperature-independent susceptibility χ_0 for $T \to 0$ between κ-H and β'-Sb.

	t'/t	J/k_B (K)	χ_0 (emu/mol)
κ-H	1.48[a] [30]	80–100	1.2×10^{-3}
β'-Sb	0.78–0.81[b] [31,32]	220–250 [17]	0.4×10^{-3} [27]

[a]Extended Hückel method calculations
[b]Density functional theory calculations

Despite the fact that the spinons are neutral in charge, their thermal Hall response κ_{xy} driven by the Lorentz force has been predicted [47]. This is a consequence of the coupling of the internal gauge flux to the external magnetic field. In the case of β'-Sb, however, no response has been observed experimentally [26]. The disagreement could be explained by the paired QSL states emerging from the instability of the Fermi sea [44–46], the QSL state with Majorana-fermion excitations [49], or the instability of the uniform flux states against the external field [48]. In the case of the former two states, finite $D(E_F)$ is interpreted by the impurity scattering effect, which seems inconsistent with $D(E_F)$ being of the correct order as determined by the value of J and the theory of a spinon Fermi surface [9].

There has been a recent theoretical study of the Hubbard model of an anisotropic triangular lattice with ring-exchange interactions [50], in addition to many studies on the Heisenberg model (see, for example, Refs. [6–9,51,52]). The Hubbard model predicts a QSL state in a limited range, $0.71 < t'/t < 1$ [50], but is inconsistent with our discovery for κ-H: the presence of QSL even for $t'/t \sim 1.48$.

Finally, we briefly mention the phase shift of the torque curve. Such a shift was not observed for β'-Sb [27]. Considering that the phase shift shows little sample dependence (see Supplemental Material [43]), it must be intrinsic to κ-H. The phase shift is considered to be of magnetic origin, as θ_0 is modified not only by the cooling, but also by the application of the magnetic field. We do not presently understand the origin of the phase shift. This remains a future problem.

In conclusion, we unveiled the third candidate for QSL states in organic spin-1/2 triangular lattices, κ-H. The QSL state was characterized by gapless magnetic excitations, similar to the case for β'-Sb. A comparative argument for κ-H and β'-Sb led us to suggest that, regardless of t'/t, the gapless QSL states share the same mechanism, that is, the

formation of a band with a Fermi surface possibly attributed to spinons.

This work is partly supported by JSPS KAKENHI under Grants No. 24340074, No. 25620052, and No. 25400384.

[1] P. W. Anderson, Mater. Res. Bull. **8**, 153 (1973).
[2] P. A. Lee, Science **321**, 1306 (2008).
[3] B. Normand, Contemp. Phys. **50**, 533 (2009).
[4] L. Balents, Nature (London) **464**, 199 (2010).
[5] B. Lake, D. A. Tennant, C. D. Frost, and S. E. Nagler, Nat. Mater. **4**, 329 (2005).
[6] Y. Hayashi, and M. Ogata, J. Phys. Soc. Jpn. **76**, 053705 (2007).
[7] M. Q. Weng, D. N. Sheng, Z. Y. Weng, and R. J. Bursill, Phys. Rev. B **74**, 012407 (2006).
[8] W. LiMing, G. Misguich, P. Sindzingre, and C. Lhuillier, Phys. Rev. B **62**, 6372 (2000).
[9] O. I. Motrunich, Phys. Rev. B **72**, 045105 (2005).
[10] M. S. Block, D. N. Sheng, O. I. Motrunich, and M. P. A. Fisher, Phys. Rev. Lett. **106**, 157202 (2011).
[11] S. S. Lee, and P. A. Lee, Phys. Rev. Lett. **95**, 036403 (2005).
[12] L. Dang, S. Inglis, and R. G. Melko, Phys. Rev. B **84**, 132409 (2011).
[13] H. Morita, S. Watanabe, and M. Imada, J. Phys. Soc. Jpn. **71**, 2109 (2002).
[14] R. Moessner, and S. L. Sondhi, Phys. Rev. Lett. **86**, 1881 (2001).
[15] Y. Qi, C. Xu, and S. Sachdev, Phys. Rev. Lett. **102**, 176401 (2009).
[16] Y. Shimizu, K. Miyagawa, K. Kanoda, M. Maesato, and G. Saito, Phys. Rev. Lett. **91**, 107001 (2003).
[17] T. Itou, A. Oyamada, S. Maegawa, M. Tamura, and R. Kato, Phys. Rev. B **77**, 104413 (2008).
[18] H. D. Zhou, E. S. Choi, G. Li, L. Balicas, C. R. Wiebe, Y. Qiu, J. R. D. Copley, and J. S. Gardner, Phys. Rev. Lett. **106**, 147204 (2011).
[19] J. G. Cheng, G. Li, L. Balicas, J. S. Zhou, J. B. Goodenough, C. Xu, and H. D. Zhou, Phys. Rev. Lett. **107**, 197204 (2011).
[20] T. H. Han, J. S. Helton, S. Chu, D. G. Nocera, J. A. Rodriguez-Rivera, C. Broholm, and Y. S. Lee, Nature (London) **492**, 406 (2012).
[21] Y. Okamoto, M. Nohara, H. Aruga-Katori, and H. Takagi, Phys. Rev. Lett. **99**, 137207 (2007).
[22] T. Itou, A. Oyamada, S. Maegawa, and R. Kato, Nat. Phys. **6**, 673 (2010).
[23] S. Yamashita, T. Yamamoto, Y. Nakazawa, M. Tamura, and R. Kato, Nat. Commun. **2**, 275 (2011).
[24] S. Yamashita, Y. Nakazawa, M. Oguni, Y. Oshima, H. Nojiri, Y. Shimizu, K. Miyagawa, and K. Kanoda, Nat. Phys. **4**, 459 (2008).
[25] F. L. Pratt, P. J. Baker, S. J. Blundell, T. Lancaster, S. Ohira-Kawamura, C. Baines, Y. Shimizu, K. Kanoda, I. Watanabe, and G. Saito, Nature (London) **471**, 612 (2011).
[26] M. Yamashita, N. Nakata, Y. Senshu, M. Nagata, H. M. Yamamoto, R. Kato, T. Shibauchi, and Y. Matsuda, Science **328**, 1246 (2010).
[27] D. Watanabe, M. Yamashita, S. Tonegawa, Y. Oshima, H. M. Yamamoto, R. Kato, I. Sheikin, K. Behnia, T. Terashima, S. Uji, T. Shibauchi, and Y. Matsuda, Nat. Commun. **3**, 1090 (2012).
[28] M. Yamashita, N. Nakata, Y. Kasahara, T. Sasaki, N. Yoneyama, N. Kobayashi, S. Fujimoto, T. Shibauchi, and Y. Matsuda, Nat. Phys. **5**, 44 (2009).
[29] S. Nakajima, T. Suzuki, Y. Ishii, K. Ohishi, I. Watanabe, T. Goto, A. Oosawa, N. Yoneyama, N. Kobayashi, F. L. Pratt, and T. Sasaki, J. Phys. Soc. Jpn. **81**, 063706 (2012).
[30] T. Isono, H. Kamo, A. Ueda, K. Takahashi, A. Nakao, R. Kumai, H. Nakao, K. Kobayashi, Y. Murakami, and H. Mori, Nat. Commun. **4**, 1344 (2013).
[31] K. Nakamura, Y. Yoshimoto, and M. Imada, Phys. Rev. B **86**, 205117 (2012).
[32] T. Tsumuraya, H. Seo, M. Tsuchizu, R. Kato, and T. Miyazaki, J. Phys. Soc. Jpn. **82**, 033709 (2013).
[33] E. P. Scriven, and B. J. Powell, Phys. Rev. Lett. **109**, 097206 (2012).
[34] H. O. Jeschke, M. deSouza, R. Valentí, R. S. Manna, M. Lang, and J. A. Schlueter, Phys. Rev. B **85**, 035125 (2012).
[35] H. C. Kandpal, I. Opahle, Y. Z. Zhang, H. O. Jeschke, and R. Valentí, Phys. Rev. Lett. **103**, 067004 (2009).
[36] H. Kamo, A. Ueda, T. Isono, K. Takahashi, and H. Mori, Tetrahedron Lett. **53**, 4385 (2012).
[37] C. Rossel, P. Bauer, D. Zech, J. Hofer, M. Willemin, and H. Keller, J. Appl. Phys. **79**, 8166 (1996).
[38] N. Elstner, R. R. P. Singh, and A. P. Young, Phys. Rev. Lett. **71**, 1629 (1993).
[39] M. Tamura and R. Kato, J. Phys. Condens. Matter **14**, L729 (2002).
[40] Z. Guguchia, S. Bosma, S. Weyeneth, A. Shengelaya, R. Puzniak, Z. Bukowski, J. Karpinski, and H. Keller, Phys. Rev. B **84**, 144506 (2011).
[41] T. Sasaki, H. Uozaki, S. Endo, and N. Toyota, Synth. Met. **120**, 759 (2001).
[42] The results of the electron-paramagnetic-resonance (EPR) study onκ-H will be reported elsewhere.
[43] See Supplemental Material at http://link.aps.org/supplemental/10.1103/PhysRevLett.112.177201 for the estimation method of the susceptibility from the torque magnetometry and the comparison among the three distinct samples.
[44] S. S. Lee, P. A. Lee, and T. Senthil, Phys. Rev. Lett. **98**, 067006 (2007).
[45] V. Galitski, and Y. B. Kim, Phys. Rev. Lett. **99**, 266403 (2007).
[46] T. Grover, N. Trivedi, T. Senthil, and P. A. Lee, Phys. Rev. B **81**, 245121 (2010).
[47] H. Katsura, N. Nagaosa, and P. A. Lee, Phys. Rev. Lett. **104**, 066403 (2010).
[48] O. I. Motrunich, Phys. Rev. B **73**, 155115 (2006).
[49] R. R. Biswas, L. Fu, C. R. Laumann, and S. Sachdev, Phys. Rev. B **83**, 245131 (2011).
[50] M. Holt, B. J. Powell, and J. Merino, Phys. Rev. Lett. (to be published).
[51] O. A. Starykh, and L. Balents, Phys. Rev. Lett. **98**, 077205 (2007).
[52] S. Ghamari, C. Kallin, S. S. Lee, and E. S. Sørensen, Phys. Rev. B **84**, 174415 (2011).